Novel magnetoresistance effect in layered magnetic structures: Theory and experiment

J. Barnaś,* A. Fuss, R. E. Camley,† P. Grünberg, and W. Zinn
Kernsforschungsanlage GmbH, Institut für Festkörperforschung, Postfach 1913, 5170 Jülich, West Germany

(Received 7 November 1989; revised manuscript received 26 April 1990)

We study magnetoresistivity in ferromagnetic-nonmagnetic multilayers both theoretically and experimentally. The theoretical approach uses a Boltzmann equation with spin-dependent bulk and interface scattering. We show that the resistivity increases when the magnetizations of the ferromagnetic films rotate from the parallel alignment to the antiparallel one. Bulk and interface contributions are studied numerically as a function of the electron mean free path and film thickness, and we show that these two effects produce characteristically different results. Experimentally we investigated both epitaxial and polycrystalline $(Fe/Cr)_n/Fe$ multilayers with $n=1$, 2, and 4. In this system the antiparallel alignment is achieved by an antiferromagnetic coupling between the Fe layers across the Cr interlayer. We also found large magnetoresistance effects in Co/Au/Co structures where the antiparallel alignment of the Co magnetizations was obtained by different coercive fields in the two Co films. A detailed comparison of the theoretical and experimental results for epitaxial Fe/Cr structures shows good agreement.

I. INTRODUCTION

Electrical transport properties of nonmagnetic metallic thin films and multilayers grown by molecular-beam epitaxy (MBE) on insulating or semiconducting substrates have been studied experimentally and theoretically by many authors.[1–11] The interest in such systems is stimulated by possible applications in microelectronic devices. Electron transport in layered systems is modified, as compared to the bulk, by additional scattering of electrons at free surfaces and interfaces. A theoretical approach to this problem, based on the Boltzmann transport equation with appropriate boundary conditions, has turned out to be very useful and satisfactory.

Very recently the transport properties of MBE-grown magnetic multilayers[12–17] and single films[18–20] have also been investigated and have revealed a range of interesting and attractive features resulting from the interplay of electronic and magnetic properties. For example, in Refs. 12 and 13 the magnetoresistivity of $(Au/Co)_n$ multilayers was investigated in the case of ultrathin Co films with perpendicular magnetic anisotropy. Despite the fact that the resistivity was essentially determined by the relatively thick Au films, the magnetic behavior of the Co films was clearly seen in the magnetoresistance. The Co films introduce some electron scattering that is strongly dependent on their magnetic state.

Very interesting magnetoresistivity phenomena have recently been found in epitaxial Fe/Cr superlattices[14] and sandwich structures.[15,16] As is well known[21,22] in the Fe/Cr multilayers there is an effective exchange coupling between neighboring Fe films for sufficiently small Cr film thickness d_0. This coupling varies from ferromagnetic at $d_0 < d_c$ to antiferromagnetic at $d_0 > d_c$, where d_c depends on the preparation conditions and is usually of the order of few Å ($d_c \approx 4$–7 Å).[16] The coupling finally vanishes for d_0 greater than about 20 Å. If the coupling is antiferromagnetic then, in zero external magnetic field, the neighboring Fe films are magnetized antiparallel. When a strong enough magnetic field is applied in the film plane, the antiferromagnetic coupling may be overcome and the magnetic moments of all Fe films can be forced to lie in the same direction. It has been found[14–16] that the resistance decreases when the film magnetizations rotate from the antiferromagnetic alignment to the ferromagnetic one. The decrease was about 1.5% in sandwich structures at room temperature[15] and about 50% in superlattices at helium temperature.[14] A mechanism that is responsible for this change in resistivity is thus strongly dependent on the magnetic state of the neighboring Fe films.

The problem seems to be similar, to some extent, to that of electron scattering from domain walls, which also leads to negative magnetoresistivity, as discussed by Cabrera and Falicov.[23] Their results, however, cannot explain the present experimental data. The mechanism considered by them gives no change in resistivity in the geometry where the current flows parallel to the domain wall and parallel (or antiparallel) to the magnetizations. Experimentally it has been shown that the large magnetoresistance effect in layered systems is nearly the same for current flowing parallel or perpendicular to the magnetizations,[14–16] and the small difference can be attributed to the magnetoresistivity anisotropy effect.

In a recent paper[24] a simple theoretical model for the description of the effect has been proposed, which is based on the phenomenological Fuchs-Sondheimer theory[25,26] with a spin-dependent interface electron scattering. The basic assumption underlying the description is that roughness of the Fe-Cr interfaces produces some spin-dependent diffusive electron scattering that is very similar to the spin-dependent impurity scattering in magnetic Fe_xCr_{1-x} alloys.[27] This spin asymmetry results from the corresponding asymmetry in the density of

states for spin-up and spin-down electrons. Although the description includes many simplifications, it reproduces all general trends of the effect, particularly its temperature and film-thickness dependence, as well as its dependence on the number of interlayers.

In this paper we extend the theoretical description of the magnetoresistance resulting from the transition from antiparallel–to–parallel arrangement of the film magnetizations in multilayer structures. In addition to the interface scattering considered earlier, we also include a bulk contribution to the effect, which may occur in systems in which the intrinsic bulk mean free path (MFP) of electrons in ferromagnetic layers is spin dependent. This may be the case in some pure ferromagnetic metals, particularly Ni. This also takes place when the ferromagnetic metal contains some impurities that lead to spin-dependent electron scattering.[27]

We also present here some new experimental data for the magnetoresistance in epitaxial and polycrystalline $(Fe/Cr)_n/Fe$ multilayers with $n=1$, 2, and 4 Cr interlayers, including the temperature dependence of the effect. In addition, we report on magnetoresistivity in Co/Au/Co structures, where the antiparallel alignment was achieved by different coercive fields of both Co films and not by an antiferromagnetic exchange coupling between the ferromagnetic films, as in the case of the Fe/Cr-layered structures.

The remainder of this paper is as follows. In Sec. II the theoretical model is described and the basic formulas for the magnetoresistance are derived. Some numerical data are presented and discussed in Sec. III. The experimental data of the magnetoresistance in Fe/Cr-layered structures, both epitaxial and polycrystalline, are presented in Sec. IV. In Sec. V we show data for the Co/Cu/Co system, with the antiparallel arrangement obtained by different coercive fields. In Sec. VI we discuss the basic results and present a detailed comparison of the theoretical calculations, with the experimental data obtained in epitaxial Fe/Cr structures.

II. THEORETICAL DESCRIPTION

Consider a layered structure consisting of two identical ferromagnetic layers, magnetized in the film plane and separated from one another by a nonmagnetic (or antiferromagnetic) spacer, as shown schematically in Fig. 1. The corresponding film thicknesses are d ($d=b-a$) and d_0 ($d_0=2a$) for the ferromagnetic films and interlayer, respectively, where a and b are defined in Fig. 1. An electric field E is applied in the film plane, along the axis x of the coordinate system. The axis z of this system is normal to the film plane.

If there is an antiferromagnetic exchange coupling between the layers across the interlayer then the magnetizations will be antiparallel for small values of the external magnetic field. If the magnetic films are exchange decoupled and have different coercive fields then the antiparallel alignment can be obtained by applying a proper external field. If the magnetic fields are coupled by an antiferromagnetic exchange interaction then the magnetizations of both layers are not spatially uniform, in the general

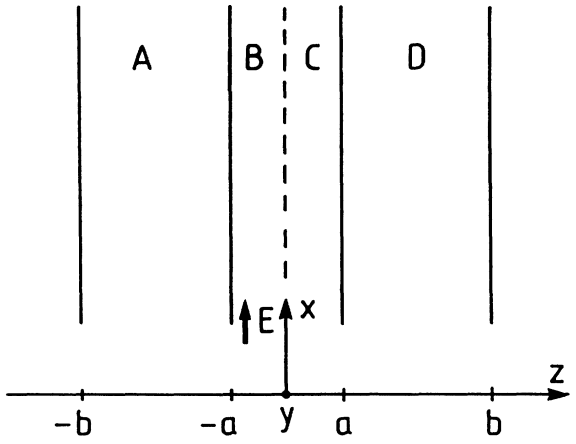

FIG. 1. Geometry of a double-layer structure and the coordinate system used in theoretical description. The broken line corresponds to a plane at which the spin quantization axis is changed.

case.[28] The uniform state occurs only in zero magnetic field, with strictly antiparallel alignment or in a sufficiently strong magnetic field that forces a uniform parallel arrangement. In our considerations, however, we neglect this small nonuniformity. We assume a uniform magnetization in each layer at arbitrary magnetic field. This assumption is quite reasonable when the interlayer exchange coupling is much weaker than the corresponding bulk one, which is just the case in the relevant experiments discussed below. In the general case, we assume that the angle θ between the magnetizations of both layers is quite arbitrary. The angle θ can be determined by minimizing the sum of the exchange, anisotropy, and Zeeman energies for the multilayer structure.

If the quantum corrections to the conductivity are negligible, the electron transport in thin metallic films can be described in terms of the Fuchs-Sondheimer theory, which includes the diffusive electron scattering on surface inhomogeneities by appropriate boundary conditions.[25,26] This phenomenological theory was successfully applied to many different problems, including transport in multilayers with or without an external magnetic field.[26]

To describe the electron transport in our systems, we extend the Fuchs-Sondheimer theory by including spin-dependent electron scattering inside the ferromagnetic films and at the interfaces. As is well known, the electron transport in magnetic $3d$ metals is described by a two-current model that takes into account a difference in scattering rates (or mean free paths) for spin-up and spin-down electrons.[27] This spin asymmetry is particularly strong in some magnetic alloys, where the ratio of the scattering rates for both spins can be of the order of 10. In the simplest approximation one may neglect any mixing of the two currents by spin-flip processes. This approximation seems to be reasonable at least at low temperatures. Similar spin asymmetry will be assumed here for the interface scattering.

In each layer the electric current is determined by the appropriate distribution functions for electrons with spin up and spin down and with the velocity $\mathbf{v}$, $f^{\uparrow(\downarrow)}(z,\mathbf{v})$, which depend only on the z component of the position vector because of the translational symmetry in the film plane. Following the general formalism, we decompose the distribution functions into two parts; the equilibrium (in zero electric field) distribution function $f_0(\mathbf{v})$ and a small contribution $g^{\uparrow(\downarrow)}(z,\mathbf{v})$ induced by external fields:

$$f^{\uparrow(\downarrow)}(z,\mathbf{v})=f_0(\mathbf{v})+g^{\uparrow(\downarrow)}(z,\mathbf{v}) . \tag{1}$$

By substituting Eq. (1) into the Boltzmann equation and considering only first-order terms, we obtain an equation for $g^{\uparrow(\downarrow)}(z,\mathbf{v})$ in each layer:

$$\frac{\partial g^{\uparrow(\downarrow)}(z,\mathbf{v})}{\partial z}+\frac{g^{\uparrow(\downarrow)}(z,\mathbf{v})}{\tau^{\uparrow(\downarrow)}v_z}=\frac{eE}{mv_z}\frac{\partial f_0(\mathbf{v})}{\partial v_x} , \tag{2}$$

where e and m denote the electron charge ($e>0$) and electron effective mass (assumed independent of the electron spin) and $\tau^{\uparrow(\downarrow)}$ are the relaxation times for spin-up and spin-down electrons. In the general case we assume that $\tau^{\uparrow}\neq\tau^{\downarrow}$ for the ferromagnetic layers. In Eq. (2) we have neglected the diamagnetic term that results from the Lorentz force. This term can lead, in general, to some interesting magnetoresistivity effects in thin films.[26] It is also responsible for a negative magnetoresistivity due to a diamagnetic deflection of the electron orbits at the domain walls.[23] These corrections, however, depend strongly on the geometry and are different for all main experimental configurations.[23,26] The experimental data[14,15] considered in this paper, on the other hand, show nearly the same effect for all the basic geometries. Thus, it seems to be reasonable to neglect this term in the first approximation.

Following the general method, we divide $g^{\uparrow(\downarrow)}(z,\mathbf{v})$ in each layer into two parts; one for electrons with positive v_z, $g_+^{\uparrow(\downarrow)}(z,\mathbf{v})$, and another one for negative v_z, $g_-^{\uparrow(\downarrow)}(z,\mathbf{v})$. The general solution of Eq. (2) can be written in the form:

$$g_{\pm}^{\uparrow(\downarrow)}(z,\mathbf{v})=\frac{eE\tau^{\uparrow(\downarrow)}}{m}\frac{\partial f_0(\mathbf{v})}{\partial v_x}\times\left[1+F_{\pm}^{\uparrow(\downarrow)}(\mathbf{v})\exp\left[\frac{\mp z}{\tau^{\uparrow(\downarrow)}|v_z|}\right]\right] , \tag{3}$$

where $F_{\pm}^{\uparrow(\downarrow)}(\mathbf{v})$ are arbitrary functions of the electron velocity $\mathbf{v}$, which are to be determined from the appropriate boundary conditions as described below.

The quantization axis for the electron spin in the ferromagnetic layer is equivalent to the corresponding static magnetization axis. When an electron crosses the interlayer, we have thus to take into account the change of the quantization direction. One can do this by introducing a plane in the middle of the interlayer, at which the quantization direction is changed. Thus, the quantization axis in the regions denoted in Fig. 1 as A and B is parallel to the static magnetization in the left layer (region A) and the quantization axis in the regions C and D is parallel to the magnetization direction in the right layer (region D). In each of the four regions A, B, C, and D one can write Eq. (3) with the corresponding functions $F_{A\pm}^{\uparrow(\downarrow)}$, $F_{B\pm}^{\uparrow(\downarrow)}$, $F_{C\pm}^{\uparrow(\downarrow)}$, and $F_{D\pm}^{\uparrow(\downarrow)}$. To determine these functions we apply the Fuchs boundary conditions at the free surfaces:

$$g_{A+}^{\uparrow(\downarrow)}=p_A^{\uparrow(\downarrow)}g_{A-}^{\uparrow(\downarrow)} \quad \text{at } z=-b , \tag{4}$$

$$g_{D-}^{\uparrow(\downarrow)}=p_D^{\uparrow(\downarrow)}g_{D+}^{\uparrow(\downarrow)} \quad \text{at } z=b , \tag{5}$$

where $p_A^{\uparrow(\downarrow)}$ and $p_D^{\uparrow(\downarrow)}$ are the Fuchs specularity factors which, in general, may also be spin dependent. The z and $\mathbf{v}$ dependence of the g functions in Eqs. (4) and (5) is not written explicitly, and it will also be dropped in the boundary conditions described below. For simplicity we have neglected any regular dependence of the specularity coefficients $p_A^{\uparrow(\downarrow)}$ and $p_D^{\uparrow(\downarrow)}$.

At the interfaces between the ferromagnetic films and the interlayer the boundary conditions can be written in the form:

$$g_{A-}^{\uparrow(\downarrow)}=T^{\uparrow(\downarrow)}g_{B-}^{\uparrow(\downarrow)}+R^{\uparrow(\downarrow)}g_{A+}^{\uparrow(\downarrow)} \quad \text{at } z=-a , \tag{6}$$

$$g_{B+}^{\uparrow(\downarrow)}=T^{\uparrow(\downarrow)}g_{A+}^{\uparrow(\downarrow)}+R^{\uparrow(\downarrow)}g_{B-}^{\uparrow(\downarrow)} \quad \text{at } z=-a , \tag{7}$$

$$g_{D+}^{\uparrow(\downarrow)}=T^{\uparrow(\downarrow)}g_{C+}^{\uparrow(\downarrow)}+R^{\uparrow(\downarrow)}g_{D-}^{\uparrow(\downarrow)} \quad \text{at } z=a , \tag{8}$$

$$g_{C-}^{\uparrow(\downarrow)}=T^{\uparrow(\downarrow)}g_{D-}^{\uparrow(\downarrow)}+R^{\uparrow(\downarrow)}g_{C+}^{\uparrow(\downarrow)} \quad \text{at } z=a , \tag{9}$$

where $T^{\uparrow(\downarrow)}$ and $R^{\uparrow(\downarrow)}$ are the coefficients of a nondiffusive (specular) transmission and a reflection of electrons at the interface between the regions A and B, as well as between the regions C and D. We have neglected any angular dependence of these coefficients. We also neglect the diffraction effects that may occur when the electron Fermi velocities in both materials are different. Apart from this, we have assumed the same transmission and reflection coefficients for electrons incident on the interfaces from the left and right sides. The later assumption is reasonable for metals having comparable work functions.

At the fictitious interface at $z=0$ one can write

$$g_{C+}^{\uparrow(\downarrow)}=\cos^2(\theta/2)g_{B+}^{\uparrow(\downarrow)}+\sin^2(\theta/2)g_{B+}^{\downarrow(\uparrow)} \quad \text{at } z=0 , \tag{10}$$

$$g_{B-}^{\uparrow(\downarrow)}=\cos^2(\theta/2)g_{C-}^{\uparrow(\downarrow)}+\sin^2(\theta/2)g_{C-}^{\downarrow(\uparrow)} \quad \text{at } z=0 , \tag{11}$$

where θ is the angle between both spin quantization directions, i.e., between the magnetization axes.

Equations (4)–(11) form a complete system of boundary conditions. By taking Eq. (3) into account one can write them in the following form:

$$c^{\uparrow(\downarrow)}F_{A+}^{\uparrow(\downarrow)}-(p_A^{\uparrow(\downarrow)}/c^{\uparrow(\downarrow)})F_{A-}^{\uparrow(\downarrow)}=p_A^{\uparrow(\downarrow)}-1 , \tag{12}$$

$$c^{\uparrow(\downarrow)}F_{D-}^{\uparrow(\downarrow)}-(p_D^{\uparrow(\downarrow)}/c^{\uparrow(\downarrow)})F_{D+}^{\uparrow(\downarrow)}=p_D^{\uparrow(\downarrow)}-1 , \tag{13}$$

$$R^{\uparrow(\downarrow)}d_1^{\uparrow(\downarrow)}F_{A+}^{\uparrow(\downarrow)}+(T^{\uparrow(\downarrow)}y^{\uparrow(\downarrow)}/d_2)F_{B-}^{\uparrow(\downarrow)}-(1/d_1^{\uparrow(\downarrow)})F_{A-}^{\uparrow(\downarrow)}=1-R^{\uparrow(\downarrow)}-y^{\uparrow(\downarrow)}T^{\uparrow(\downarrow)} , \tag{14}$$

$$(R^{\uparrow(\downarrow)}y^{\uparrow(\downarrow)}/d_2)F_{B-}^{\uparrow(\downarrow)}+T^{\uparrow(\downarrow)}d_1^{\uparrow(\downarrow)}F_{A+}^{\uparrow(\downarrow)}-y^{\uparrow(\downarrow)}d_2F_{B+}^{\uparrow(\downarrow)}=y^{\uparrow(\downarrow)}-R^{\uparrow(\downarrow)}y^{\uparrow(\downarrow)}-T^{\uparrow(\downarrow)}\ , \tag{15}$$

$$R^{\uparrow(\downarrow)}d_1^{\uparrow(\downarrow)}F_{D-}^{\uparrow(\downarrow)}-(T^{\uparrow(\downarrow)}y^{\uparrow(\downarrow)}/d_2)F_{C-}^{\uparrow(\downarrow)}-(1/d_1^{\uparrow(\downarrow)})F_{D+}^{\uparrow(\downarrow)}=1-R^{\uparrow(\downarrow)}-y^{\uparrow(\downarrow)}T^{\uparrow(\downarrow)}\ , \tag{16}$$

$$(R^{\uparrow(\downarrow)}y^{\uparrow(\downarrow)}/d_2)F_{C+}^{\uparrow(\downarrow)}+T^{\uparrow(\downarrow)}d_1^{\uparrow(\downarrow)}F_{D-}^{\uparrow(\downarrow)}-y^{\uparrow(\downarrow)}d_2F_{C-}^{\uparrow(\downarrow)}=y^{\uparrow(\downarrow)}-y^{\uparrow(\downarrow)}R^{\uparrow(\downarrow)}-T^{\uparrow(\downarrow)}\ , \tag{17}$$

$$\cos^2(\theta/2)F_{B+}^{\uparrow(\downarrow)}+\sin^2(\theta/2)F_{B+}^{\downarrow(\uparrow)}-F_{C+}^{\uparrow(\downarrow)}=0\ , \tag{18}$$

$$\cos^2(\theta/2)F_{C-}^{\uparrow(\downarrow)}+\sin^2(\theta/2)F_{C-}^{\uparrow(\downarrow)}-F_{B-}^{\uparrow(\downarrow)}=0\ , \tag{19}$$

where the $\mathbf{v}$ dependence of the F functions is not written explicitly, and the parameters $c^{\uparrow(\downarrow)}$, $d_1^{\uparrow(\downarrow)}$, and d_2 are defined as

$$c^{\uparrow(\downarrow)}=\exp(b/\lambda_1^{\uparrow(\downarrow)}\cos\beta)\ , \tag{20}$$

$$d_1^{\uparrow(\downarrow)}=\exp(a/\lambda_1^{\uparrow(\downarrow)}\cos\beta)\ , \tag{21}$$

$$d_2=\exp(a/\lambda_2\cos\beta)\ . \tag{22}$$

Here β is the angle between the z axis and the velocity $\mathbf{v}$, and $\lambda_1^{\uparrow(\downarrow)}$ is the electron MFP for spin-up (spin-down) electrons in the ferromagnetic layers

$$\lambda_1^{\uparrow(\downarrow)}=v_{F1}\tau_1^{\uparrow(\downarrow)}\ , \tag{23}$$

with v_{F1} and $\tau_1^{\uparrow(\downarrow)}$ being the Fermi velocity (assumed the same for both spin directions) and the corresponding relaxation times. Similarly, λ_2 is here the electron MFP in the interlayer

$$\lambda_2=v_{F2}\tau_2\ , \tag{24}$$

with v_{F2} and τ_2 being the corresponding Fermi velocity and relaxation time. The parameters $y^{\uparrow(\downarrow)}$ in Eqs. (12)–(17) take into account the difference in the electronic properties of both materials (ferromagnetic films and interlayer) and are defined as

$$y^{\uparrow}=\tfrac{1}{2}rs(1+N_b)\ , \tag{25}$$

$$y^{\downarrow}=\tfrac{1}{2}rs(1+1/N_b)\ , \tag{26}$$

where

$$N_b=\lambda_1^{\downarrow}/\lambda_1^{\uparrow}\ , \tag{27}$$

$$r=2\lambda_2/(\lambda_1^{\downarrow}+\lambda_1^{\uparrow})\ , \tag{28}$$

$$s=m_1v_{F1}/m_2v_{F2}\ , \tag{29}$$

with m_1 and m_2 being the effective electron mass in magnetic layers and interlayer, respectively. The parameter N_b describes the spin asymmetry of the bulk scattering rate in the ferromagnetic material. Equations (12)–(19) determine all of the unknown F functions and, consequently, the electron distribution function, and current density. As the coefficients in Eqs. (12)–(19) only depend on the angle between the velocity and the z axis, i.e., on β, the F functions can also be considered as functions of β, $F(\mathbf{v})\rightarrow F(\beta)$. In the following, Eqs. (12)–(19) will only be solved numerically.

The total current I (per unit length along the y axis) is given by the general equation

$$I=-e\int dz\int d\mathbf{v}[g^{\uparrow}(\mathbf{v},z)+g^{\downarrow}(\mathbf{v},z)]v_x\ , \tag{30}$$

where the integration over z has to be performed in each region separately. The integration over $\mathbf{v}$ can be carried out very easily assuming the degenerate electron gas. Finally, one can write the expression for the current I in the following form:

$$I=\sigma_1 d_t\chi E\ , \tag{31}$$

where σ_1 is the bulk conductivity of the ferromagnetic material

$$\sigma_1=\sigma_1^{\uparrow}+\sigma_1^{\downarrow}\ , \tag{32}$$

d_t is the total thickness of the sandwich

$$d_t=2d+d_0\ , \tag{33}$$

and χ is defined as follows:

$$\chi=1+(\mu-1)d_0/d_t+(\tfrac{3}{8}d_t)\int_0^{\pi/2}d\beta h(\beta)\sin^3\beta\cos\beta\ . \tag{34}$$

The function $h(\beta)$ in the above integral is given by the following expression:

$$h(\beta)=\mu\lambda_2h_2(\beta)+(1-\eta)\lambda_1^{\uparrow}h_1^{\uparrow}(\beta)+(1+\eta)\lambda_1^{\downarrow}h_1^{\downarrow}(\beta)\ , \tag{35}$$

with

$$h_2(\beta)=(F_{B+}^{\uparrow}+F_{B-}^{\downarrow}+F_{C-}^{\uparrow}+F_{C-}^{\downarrow})(d_2-1)+(F_{B-}^{\uparrow}+F_{B-}^{\downarrow}+F_{C+}^{\uparrow}+F_{C+}^{\downarrow})(1-1/d_2)\ , \tag{36}$$

$$h_1^{\uparrow}(\beta)=(F_{A+}^{\uparrow}-F_{D-}^{\uparrow})(c^{\uparrow}-d_1^{\uparrow})+(F_{A-}^{\uparrow}+F_{D+}^{\uparrow})(1/d_1^{\uparrow}-1/c^{\uparrow})\ , \tag{37}$$

$$h_1^{\downarrow}(\beta)=(F_{A+}^{\downarrow}+F_{D-}^{\downarrow})(c^{\downarrow}-d_1^{\downarrow})+(F_{A-}^{\downarrow}-F_{D+}^{\downarrow})(1/d_1^{\downarrow}-1/c^{\downarrow}\ , \tag{38}$$

where $c^{\uparrow(\downarrow)}$, $d_1^{\uparrow(\downarrow)}$, and d_2 are given by Eqs. (20)–(22) and the parameters μ and η are defined as

$$\mu=\sigma_2/\sigma_1=rts\ , \tag{39}$$

$$\eta=(\sigma_1^{\downarrow}-\sigma_1^{\uparrow})/(\sigma_1^{\downarrow}+\sigma_1^{\uparrow})=(N_b-1)/(N_b-1)\ . \tag{40}$$

In the above equations σ_2 is the bulk conductivity of the interlayer, N_b, r and s are defined by Eqs. (27)–(29), and t is the ratio of the electron concentration in the interlayer (n_2) and in the magnetic material (n_1), $t=n_2/n_1$. The β dependence of the right-hand side of Eqs. (36)–(38) is contained in the F functions, as discussed above.

The resistivity ρ of the system is then given by

$$\rho = 1/\sigma_1 \chi \ . \tag{41}$$

The relative change of the resistivity at the transition from $\theta \neq 0$ to $\theta = 0$ (parallel alignment) is given by

$$x(\theta) = \frac{\rho|_\theta - \rho|_{\theta=0}}{\rho|_{\theta=0}} = \frac{\chi|_{\theta=0}}{\chi|_\theta} - 1 \ . \tag{42}$$

Equation (42) is the basic result for the relative magnetoresistivity in double-layer structures. The quantity x can also be expressed in terms of the magnetic field H_0 when one knows the H_0 dependence of θ. To characterize the size of the effect it is sufficient to give only an amplitude of the effect, i.e., its value when the arrangement changes from antiparallel-to-parallel alignment. This amplitude, described in the following as $(\rho^{\uparrow\downarrow} - \rho^{\uparrow\uparrow})/\rho^{\uparrow\uparrow}$, is given by $x(\theta = \pi)$:

$$(\rho^{\uparrow\downarrow} - \rho^{\uparrow\uparrow})/\rho^{\uparrow\uparrow} = x(\theta = \pi) \ , \tag{43}$$

where $\rho^{\uparrow\downarrow}$ and $\rho^{\uparrow\uparrow}$ are the resistivities with antiparallel and parallel alignment of the film magnetizations, respectively, ($\rho^{\uparrow\uparrow} = \rho|_{\theta=0}$, $\rho^{\uparrow\downarrow} = \rho|_{\theta=\pi}$).

The above considerations can be generalized easily to more complicated structures, such as multilayers with two or more interlayers. They can also be generalized to infinite periodic superlattices. In the latter case one can do this using two different methods. (1) One can write the basic equations for the elementary unit of the superlattice, consisting of two magnetic layers (with thickness d) and two interlayers (with thickness d_0), and then apply periodic boundary conditions. (2) One may consider only a three-layered structure with two magnetic layers (of thickness $d/2$) and one interlayer (of thickness d_0) and then apply the perfectly reflecting boundary conditions at the external surfaces (the specularity factors equal to 1). The later trick can also be applied to generate solutions for composed structures from solutions known for multilayers with smaller number of interlayers. We have performed appropriate calculations for multilayers with two and four interlayers (three and five magnetic layers) as well as for an infinite superlattice. The appropriate expressions are very similar to those given above and will not be presented here. We show only appropriate numerical results.

III. NUMERICAL RESULTS

As can be seen from the preceding section there are, in general, many independent parameters that enter the final formula for the relative change of the resistivity, $(\rho^{\uparrow\downarrow} - \rho^{\uparrow\uparrow})/\rho^{\uparrow\uparrow}$. Some of them are not known, and it seems to be difficult to determine them from available experimental data. We have thus to simplify the problem by some additional assumptions. At first we assume that the specular reflection coefficients $R^\uparrow$ and $R^\downarrow$ are sufficiently small[6] to be neglected in further calculations, $R^\uparrow = R^\downarrow = 0$. This assumption is reasonable if the potential step at the interface is relatively small. Since the work functions for Cr and Fe are comparable, one may expect this assumption to be correct for Fe/Cr multilayers. Apart from this, we neglect any difference between the Fuchs parameters for electrons with spin up and spin down assuming $p_A^\uparrow = p_A^\downarrow = p_D^\uparrow = p_D^\downarrow = p$.

To characterize the magnitude and basic features of the effect we neglect first any difference between the conductivities of both materials assuming $t = s = r = 1$. This assumption is reasonable when the conductivities of both constituents are comparable and the interlayer thickness is much smaller than that of the ferromagnetic layers, $d_0 \ll d$. (In the following sections, however, the difference in conductivities will be taken into account.) Thus, we have reduced the number of independent parameters to only four: $T^\uparrow$, $T^\downarrow$, N_b, and p. Instead of $T^\uparrow$ and $T^\downarrow$ we introduce the interface diffusive scattering parameters of $D^\uparrow$ and $D^\downarrow$ that are determined by $T^\uparrow$ and $T^\downarrow$ as

$$D^{\uparrow(\downarrow)} = 1 - T^{\uparrow(\downarrow)} \ , \tag{44}$$

which results from the particle conservation law and the omission of specular reflection at the interfaces. As independent parameters we assume now $D^\uparrow$, N_s, N_b, and p, where N_s is defined as the ratio of the diffusive scattering parameters for spin-up and spin-down electrons

$$N_s = D^\uparrow / D^\downarrow \ . \tag{45}$$

The parameter N_s describes the spin asymmetry of the diffusive scattering of electrons at the interfaces.

Under the above assumptions the magnetoresistivity consists of two different contributions. The first one, which we call the bulk contribution, results from the difference of the intrinsic scattering rates for spin-up and spin-down electrons in the ferromagnetic material and is described by the parameter N_b. Another contribution results from the spin-dependent interface diffusive scattering and is described by the factor N_s.

The basic problem is to determine the origin of the effect observed in Fe/Cr-layered systems.[14-16] In other words, it is interesting to consider whether the experimentally observed effect results from the interface or bulk contribution, or if it is a superposition of both of them. At first, however, we analyze numerically some basic features of each contribution separately. We assume here that the asymmetry of the scattering rates for spin-up and spin-down electrons that are diffusively scattered by the Fe-Cr interface roughness is the same as in $Fe_{1-x}Cr_x$ alloys. As is well known,[27] in this alloy the spin asymmetry is described by the factor $N_s = 6$ and results from a spin asymmetry in the density of electron states at the Fermi energy, caused by the Cr impurities. The same mechanism and number N_s is assumed to be valid for the Fe-Cr interfaces. We cannot find, however, the appropriate value of N_b for pure Fe in the relevant literature. In the following numerical calculations in this section we thus assume $N_s = 6$ and $N_b = 2$.

In Fig. 2 we present numerical results independently for the (a) bulk and (b) interface contributions to the magnetoresistivity. Here we plot the percent change in resistivity for double layers versus the arithmetic mean value λ_1 of the MFP in the ferromagnetic material

$$\lambda_1 = (\lambda_1^\uparrow + \lambda_1^\downarrow)/2 \ . \tag{46}$$

The appropriate results are shown for structures with different specularity factor p. Note, that the case $p=1$ is equivalent to the infinite superlattice with doubled thickness of the magnetic layers. With the assumed values of N_b and N_s, both contributions are comparable and they are also comparable with the experimental results. However, the MFP dependence of the bulk contribution in double layers with $p<1$ is qualitatively different from that of the interface contribution. As is seen in Fig. 2, the bulk contribution has a maximum at a well-defined MFP. For an appropriate range of p this MFP can be reached experimentally (at appropriate temperatures). Thus, the temperature dependence of the bulk contribution should also exhibit a maximum. The interface contribution, on the other hand, does not show such behavior. It always increases with decreasing temperature. This difference in temperature dependence offers a possibility to distinguish experimentally between both contributions. The experimental data of Refs. 14–16 favor the interface contribution as the dominant one.

Another possibility to distinguish experimentally between the bulk and interface contributions results from the thickness dependence of the effect. In Fig. 3 we show numerical results for the relative magnetoresistivity in double layers versus the thickness d of the magnetic films. For large d the effect decreases in both cases with increasing d. For small d the behavior is different for both contributions.

Some numerical results for the interface contribution to the magnetoresistivity have already been presented elsewhere.[24] The considerations have been restricted there to double layers and infinite superlattices. We have concluded that the comparison of the experimental and numerical calculations should allow, in principle, the determination of the two independent parameters $D^{\uparrow}$ and N_s (assuming $N_b=1$ and known specularity factor p). However, the temperature dependence of the effect in a double-layer structure is not sufficient for this, since the same magnitude of the effect for the whole relevant temperature range can be obtained with different sets of the parameters $D^{\uparrow}$ and N_s. To determine them uniquely one also has to take into account the dependence of the effect on the number of interlayers. In Fig. 4 we show the magnitude of the interface contribution to the relative magnetoresistivity in multilayers with one, two, and four interlayers and in superlattices. The numerical results are

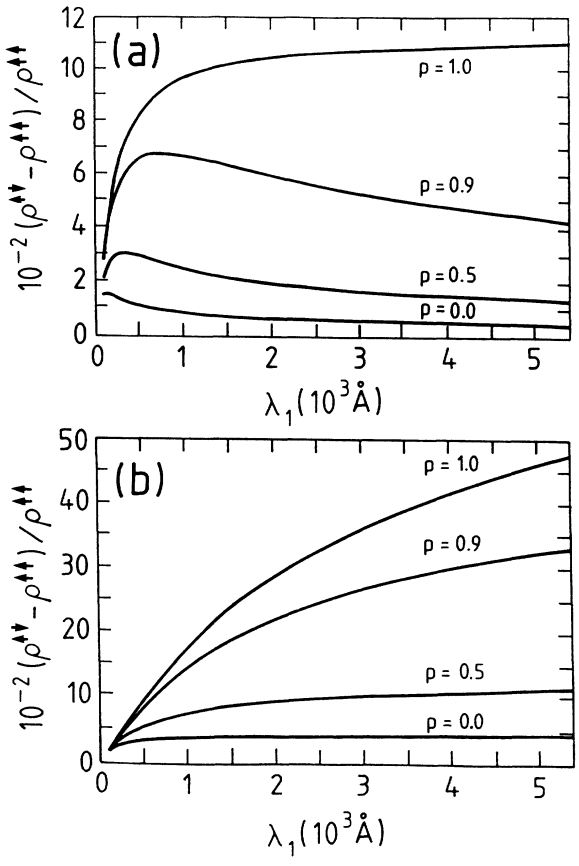

FIG. 2. (a) Bulk and (b) interface contribution to the magnetoresistivity in double layers with $d=100$ and 10 Å for different values of the specularity factor p. The curves in (a) have been calculated for $N_b=2$, $D^{\uparrow}=0$, and $r=s=t=1$, whereas the curves in (b) for $N_s=6$, $D^{\uparrow}=0.5$, $N_b=1$, and $r=s=t=1$.

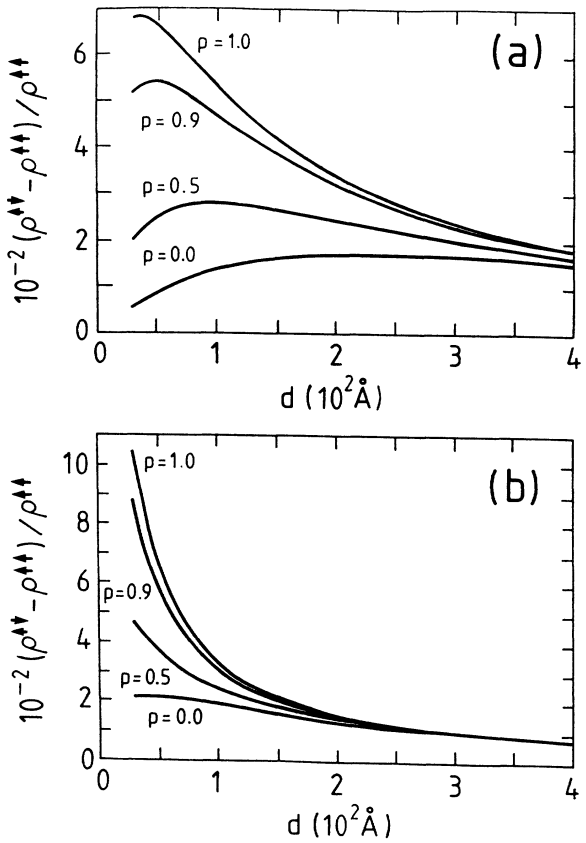

FIG. 3. (a) Bulk and (b) interface contribution to the magnetoresistivity in double layers vs thickness of the ferromagnetic layers. The curves are calculated for the specularity factors as indicated. The interlayer thickness is assumed to be constant, $d_0=10$ Å. The other parameters assumed in numerical calculations are (a) $N_b=2$, $D^{\uparrow}=0$, $\lambda_1=200$ Å, and $r=s=t=1$; (b) $N_s=6$, $D^{\uparrow}=0.5$, $N_b=1$, $\lambda_1=200$ Å, and $r=s=t=1$.

presented here for three different sets of $D^{\uparrow}$ and N_s, which give the same effect in a double-layer structure, as is shown by the lowest three curves in Fig. 4(a). One can see that the effect strongly increases with the increasing number of interlayers. Apart from this, the curves for the multilayers with more than one interlayer are well separated from each other, contrary to the case of a simple double layer. The difference increases with an increasing number of interlayers and it also increases with decreasing temperature.

To understand the increase in the size of the effect with an increasing number of layers, we note that our ratio essentially measures the magnetic-dependent scattering divided by the nonmagnetic scattering. (Of course the denominator should be all scattering, but the magnetic portion is very small). To increase this ratio, we can either increase the numerator by increasing the number of magnetic scattering events (i.e., increase the number of interfaces) or we can reduce the denominator. In the limit that the mean free path is longer than the thickness of the sample, the primary method to reduce the nonmagnetic scattering is to reduce interactions with the outer surface. Thus a thicker film has a lower resistivity. In our calculations we find both effects to be about equal in importance.

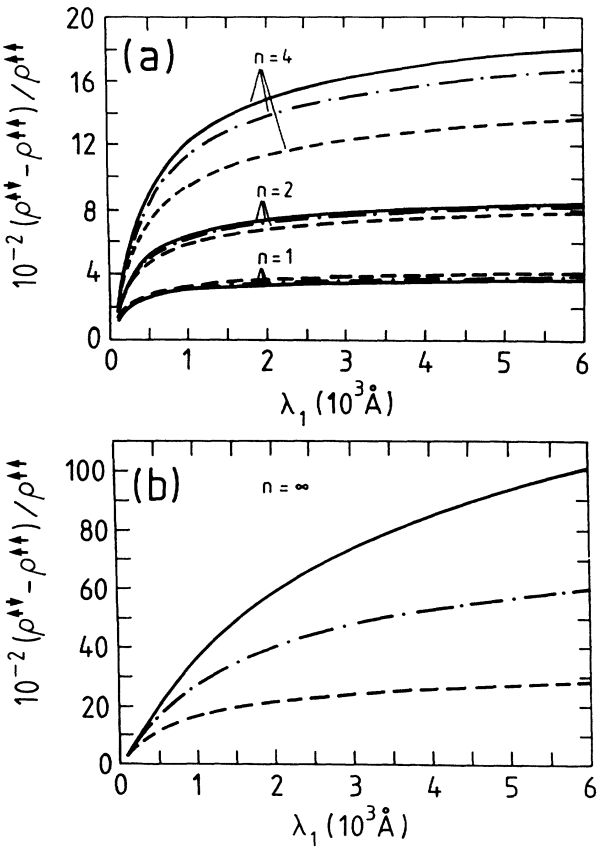

FIG. 4. (a) Interface contribution to the magnetoresistivity in multilayers with $n=1,2,4$ interlayers (b) and in superlattices, $n=\infty$, vs the MFP in the ferromagnetic material. The parameters assumed here are $N_b=1$, $d_0=7$ Å, $d=100$ Å, and $p=0$. The other parameters are $D^{\uparrow}=0.44$, $N_s=12$ (——); $D^{\uparrow}=0.48$, $N_s=6$ (—·—·—·—); $D^{\uparrow}=0.588$, $N_s=3$ (— — —).

IV. EXPERIMENTAL RESULTS FOR Fe/Cr-LAYERED STRUCTURES

Epitaxial $(Fe/Cr)_n/Fe$ samples with $n=1$, 2, and 4 and the thicknesses $d=120$ Å and $d_0=10$ Å were evaporated on [110]-oriented GaAs. Then the Fe layers grow parallel to the (110) atomic planes. The magnetic easy axis is in the film plane and is parallel to the [100] direction, whereas the in-plane hard axis is perpendicular to the easy direction. To measure resistivity the samples were prepared in the shape of a long thin stripe, with the easy axis along the stripe. Further preparational and experimental details have been published elsewhere.[15]

For the Cr-interlayer thickness of $d_0=10$ Å there is an antiferromagnetic coupling between the Fe films across the interlayer.[21,22] In zero external magnetic field the Fe films are then magnetized along the easy direction (and consequently along the stripe) and the magnetizations of the neighboring Fe films are antiparallel to one another. At a well defined and strong enough magnetic field, applied along the easy direction, the magnetizations rotate from the antiparallel alignment to the parallel one. This rotation is accompanied by a decrease in the resistivity, which is measured for currents flowing along the stripe. In both parallel and antiparallel configurations the current flows parallel (or antiparallel) to the film magnetization, so there is no change in the resistivity due to the magnetoresistivity anisotropy effect. The whole decrease of the resistivity results from the transition from antiparallel-to-parallel alignment of the Fe-film magnetizations.

In Fig. 5 we show magnetoresistance traces for the three investigated structures and for three different temperatures. The resistance of each system is plotted here as it is observed during a scan through the hysteresis loop. One can see that the resistance decreases at some external magnetic field, where the transition from antiparallel-to-parallel arrangement of the film magnetizations takes place. Further experimental data are given in Fig. 6, where the temperature dependence of the relative change of the resistivity, as defined by Eq. (43), is presented. It is clear that the effect increases with decreasing temperature and with an increasing number of the Cr interlayers. At helium temperature the relative change is about 14% for the multilayer with $n=4$ interlayers, 6.5% for the structure with $n=2$, and 4% for the double-layer system ($n=1$). The corresponding room-temperature values are 2.8, 2.1, and 1.5% for $n=4$, 2, and 1, respectively. The corresponding absolute change of the resistivity is shown in Fig. 7. It is worth noting a broad maximum in the temperature dependence of $\rho^{\uparrow\downarrow}-\rho^{\uparrow\uparrow}$, which shifts towards lower temperature with an increasing number of Cr interlayers.

We have also prepared polycrystalline Fe/Cr-layered structures that were grown on oxidized silicon. As in the case of epitaxial samples, we found an antiferromagnetic interlayer coupling between the Fe films, which occurs for appropriate range of interlayer thicknesses. The pres-

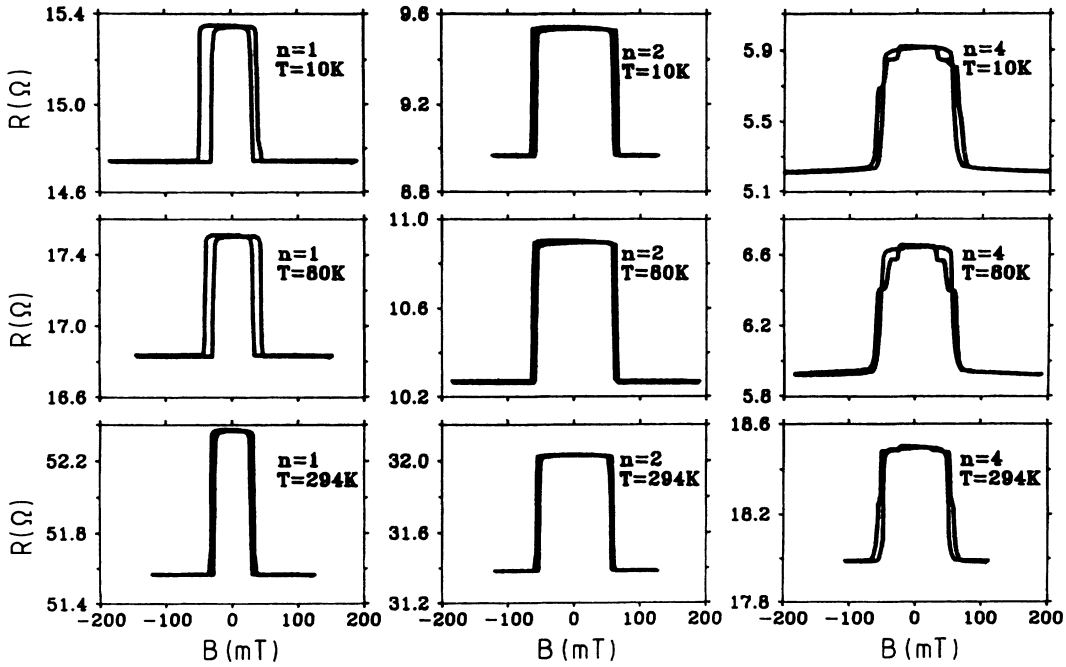

FIG. 5. Resistance of the epitaxial $(Fe/Cr)_n/Fe$ structures with antiferromagnetic interlayer coupling vs applied magnetic field for $n=1,2,4$ and for different temperatures. The thicknesses of the Fe and Cr layers are $d=120$ Å and $d_0=10$ Å, respectively. The magnetic field was applied along the flowing current. Further details are in the text.

ence of this coupling was checked, as before,[21] using the magneto-optic Kerr effect (MOKE) signal measurements and by light-scattering techniques, and its strength was found to be comparable with that in the epitaxial multilayers grown on GaAs.

The appropriate magnetoresistivity measurements in polycrystalline samples have been performed for an external magnetic field parallel and perpendicular to the flowing current. Some of the experimental results, obtained for simple double layers and multilayers with two Cr interlayers, are shown in Fig. 8 for room and helium temperature. The traces for the magnetic field parallel and perpendicular to the current differ due to the magnetoresistivity anisotropy effect. To estimate the relative change of the resistivity, which results from the rotation of the film magnetizations from the antiparallel-to-parallel alignment, one has to subtract the anisotropy contribution from the total change. The percentage change of the resistivity is then a little smaller than in the corresponding epitaxial structures.

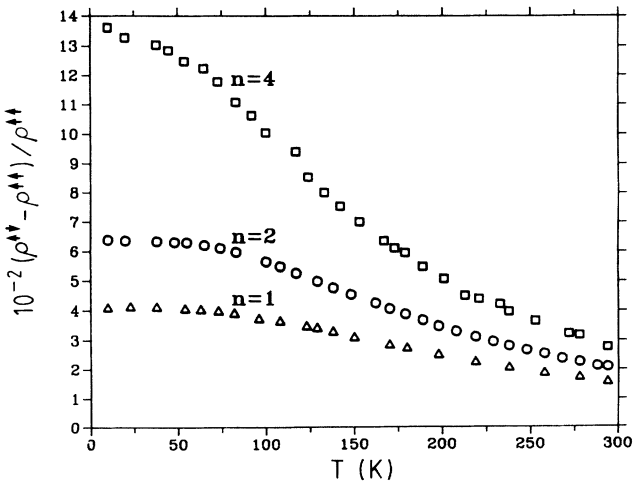

FIG. 6. Temperature dependence of the relative change of the resistivity in the epitaxial $(Fe/Cr)_n/Fe$ structures with $n=1,2,4$. Film thicknesses and other details as in Fig. 5.

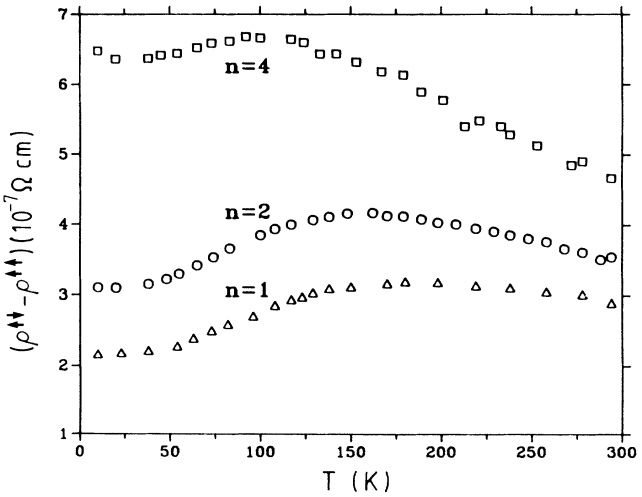

FIG. 7. Temperature dependence of the absolute change of the resistivity in epitaxial $(Fe/Cr)_n/Fe$ structures with $n=1,2,4$.

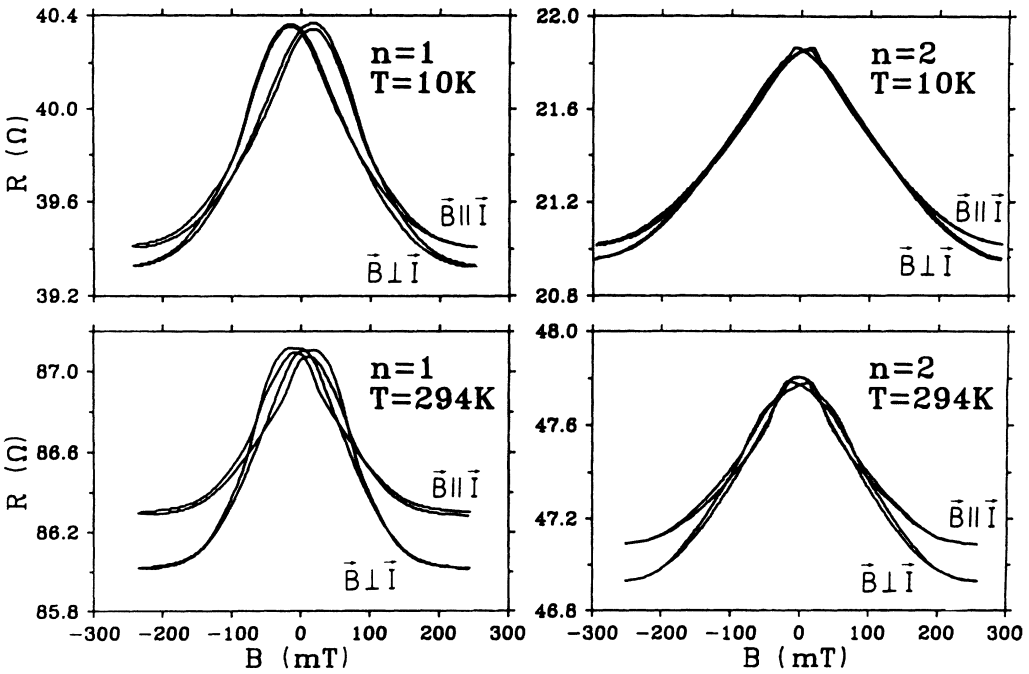

FIG. 8. Experimental traces of the resistance in polycrystalline $(Fe/Cr)_n/Fe$ structures with antiferromagnetic interlayer coupling for $n=1$ and 2 and for $d=100$ Å and $d_0=7$ Å.

V. MAGNETORESISTIVITY IN THE Co/Au/Co SYSTEM

The magnetoresistance effects investigated in this paper consist of a decrease in the resistivity when the magnetizations of the ferromagnetic layers, separated by a nonmagnetic (or antiferromagnetic) layer, rotate from antiparallel-to-parallel alignment. In the Fe/Cr-layered structures described in the preceding section, the antiparallel alignment was induced by an antiferromagnetic exchange coupling between neighboring Fe layers across the Cr interlayers. The origin of the antiparallel alignment, however, was not important for the theoretical description of the effect, which was presented in Sec. II. One may thus expect similar effects in double layers with no antiferromagnetic coupling between the ferromagnetic layers but with the antiparallel alignment obtained by other means, for example by different coercive fields of both ferromagnetic films. To analyze this problem we have fabricated Co/Au/Co double layers with the Au interlayers thick enough so there is no exchange coupling between the Co films. The first Co layer was evaporated on [110]-oriented GaAs, whereas the second one was grown on the Au interlayer. Owing to this fact, both Co films have different coercive fields. In Fig. 9(a) the hysteresis loop obtained via the magneto-optic Kerr effect (MOKE) at room temperature is shown for the Co/Au/Co structure with a Au interlayer thickness $d_0=60$ Å and Co film thickness $d=100$ Å. As one can see, there is a range of magnetic fields where the magnetizations of both Co layers are aligned antiparallel, as indicated by arrows in Fig. 9(a). In Fig. 9(b) and 9(c) we show the resistance traces as we scan through the hysteresis loop for room and low temperature. The experimental configuration here was the same as in the case of epitaxial Fe/Cr structures, i.e., the current flows parallel to an external magnetic field. At sufficiently high magnetic fields the magnetizations of both ferromagnetic films are parallel. We see that the resistivity increases each time the antiparallel alignment is achieved during a scan through the hysteresis loop. The relative change of the resistivity, defined in the same way as previously, increases with decreasing temperature. We have also investigated samples with other film thicknesses. The results show that the effect increases with a decreasing thickness of the films. The magnetoresistivity in the Co/Au-layered system has thus the same basic features as in the Fe/Cr structures.

VI. COMPARISON OF THE THEORETICAL AND EXPERIMENTAL RESULTS FOR EPITAXIAL Fe/Cr STRUCTURES AND DISCUSSION

The basic features of the effect, found experimentally are (i) the effect increases with decreasing temperature; (ii) it increases with decreasing film thickness; (iii) it increases with an increasing number of interlayers. All these features can be used for verification of the theoretical predictions with the experimental results. However, the most reliable one seems to be the temperature dependence of the effect. This follows from the fact that the relevant experiments are performed on one single sample. In the case of other features one has to compare data obtained on different samples. The basic parameters, however, are not strictly reproducible and have some statistical distribution, which makes the comparison more difficult.

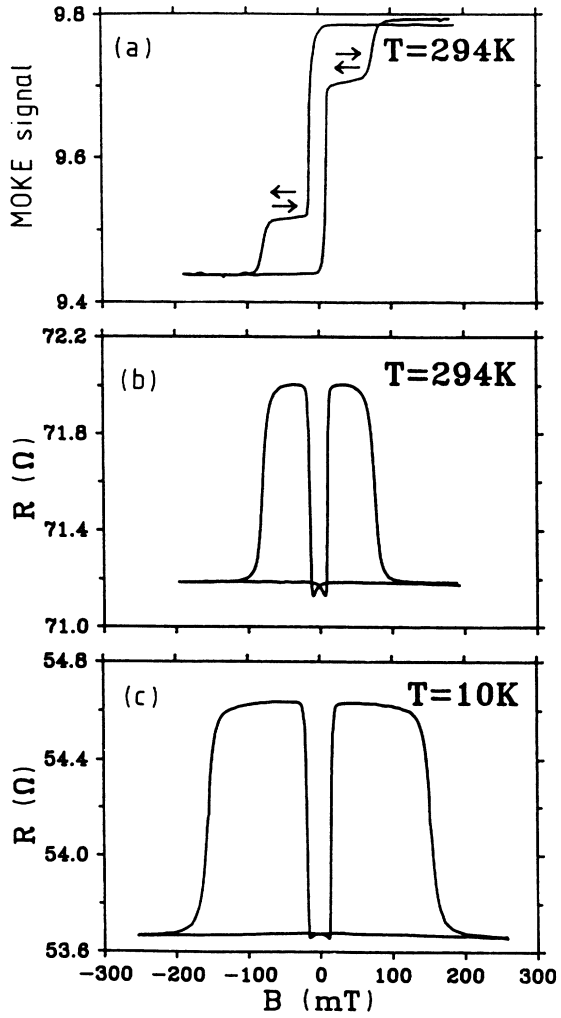

FIG. 9. (a) MOKE-signal and (b) and (c) resistance of the Co/Au/Co structure with the Co-film thickness $d=100$ Å and the Au-interlayer thickness $d_0=60$ Å.

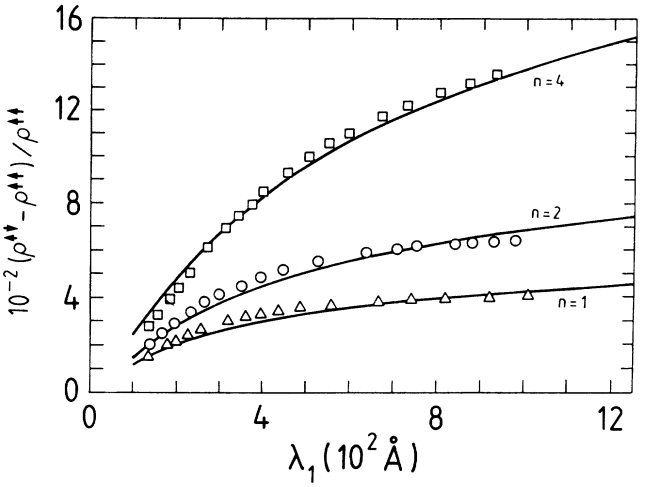

FIG. 10. Theoretical (lines) and experimental (points) magnetoresistivity in the epitaxial $(Fe/Cr)_n/Fe$ structures investigated in this paper. The experimental data of Fig. 6 are repeated here and adapted to the λ_1 scale as described in the text. In numerical calculations we assumed $N_s=6$, $N_b=1.05$, $p=0.2$, $r=2$, and $s=t=1$, and $D^{\uparrow}=0.485$ for $n=1$, $D^{\uparrow}=0.445$ for $n=2$, and $D^{\uparrow}=0.495$ for $n=4$.

In the following we present a more detailed analysis of the new magnetoresistance effect in the case of epitaxial Fe/Cr structures and compare the experimental data with the appropriate numerical calculations.

We assume for simplicity that the whole difference in the conductivities of both constituents results from the difference in the corresponding MFP's and the other electronic parameters are the same for both materials. In numerical calculations appropriate for Fe/Cr structures we assume thus $r=2$ and $s=t=1$. Apart from this, we assume $N_s=6$ according to the data obtained from Fe-Cr alloys.[14,27]

To compare theoretical predictions with the experimental data shown in Fig. 6 one has to evaluate the intrinsic electron MFP in the Fe films (the MFP in the Cr films is then determined by the parameter r). To do this we applied the following procedure. Assuming certain values for the parameters p, $D^{\uparrow}$, and N_b, and employing Eq. (41) (or its extensions for larger n) we determined the resistivity of the structure at parallel alignment of the film magnetizations as a function of the MFP. From the comparison with the experimentally found temperature dependence of the corresponding resistivity we determined MFP versus temperature. Taking into account this dependence, next we calculated [from Eq. (43)] the temperature dependence of the relative change of the resistivity. This has to be in agreement with the appropriate experimental results. One has thus to find a set of the relevant parameters which is consistent with the experimental data for $\rho^{\uparrow\uparrow}$ and $(\rho^{\uparrow\downarrow}-\rho^{\uparrow\uparrow})/\rho^{\uparrow\uparrow}$. In the appropriate calculations we assumed $\rho\lambda_1=$const and for Fe we used $\rho=9.7$ $\mu\Omega$cm and $\lambda_1=200$ Å at room temperature.[20] This assumption works very well for simple metals. It is also usually applied for transition metals. However, one has to realize that in the later case there are considerable deviations from this approximation.[4] The appropriate results for the epitaxial Fe/Cr structures investigated in this paper are shown in Fig. 10, where the lines represent theoretical results and the dots correspond to the experimental data from Fig. 6, which have been adapted to the λ_1 scale as discussed above. The agreement is satisfactory.

In the numerical calculations described above we assumed the same N_s, N_b, and p for all structures. The only parameter that was allowed to be different for different samples was $D^{\uparrow}$. The values of $D^{\uparrow}$ at which the best fit was obtained are $D^{\uparrow}=0.485$ for $n=1$, $D^{\uparrow}=0.445$ for $n=2$, and $D^{\uparrow}=0.495$ for $n=4$. These values differ from each other by less than 10%, which is quite reasonable. We note that a relatively small value for N_b is assumed for Fig. 10. The good agreement between experiment and theory indicates that for our samples interface scattering is more significant than bulk scattering.

In conclusion we may state that the simple theoretical

description of the effect, presented in this paper, gives reasonable agreement with the experimental data. A small difference between experimental and numerical results can follow from the assumed approximations, the most important of which is the assumption of a spherical Fermi surface. One has to realize that some features of the electron scattering from surface or interface inhomogeneities are not described properly by the simple Fuchs-Sondheimer theory, especially when the mean free path is much longer than the film thickness.[29] At small thicknesses one should also take into account the quantum-size effect.[30] These and related questions are planned to be analyzed in the future.

ACKNOWLEDGMENTS

The work of R.E.C. was partially supported by the U.S. Army Research Office under Grant No. DAAL03-88-K-0061.

*Permanent address: Institute of Physics, Technical University, Piotrowo 3, 60-965 Poznań, Poland.

†Permanent address: Institute of Physics, University of Colorado, Colorado Springs, Colorado 80933-7150.

[1]M. R. Khan, C. S. L. Chun, G. P. Felcher, M. Grimsditch, A. Kueny, C. M. Falco, and I. K. Schuller, Phys. Rev. B **27**, 7186 (1983).

[2]P. F. Garcia and A. Suna, J. Appl. Phys. **54**, 2000 (1983).

[3]R. Dimmich, J. Phys. F **15**, 2477 (1985).

[4]M. Gurwitch, Phys. Rev. B **34**, 540 (1986).

[5]Chu-Xing Chen, Appl. Phys. A **40**, 37 (1986); **42**, 145 (1987).

[6]J. W. C. de Vries, Solid State Commun. **65**, 201 (1988).

[7]J. W. C. de Vries and F. J. A. den Broeder, J. Phys. F **18**, 2635 (1988).

[8]M. T. Perez-Frias and J. L. Vicent, Phys. Rev. B **38**, 9503 (1988).

[9]M. Jałochowski and E. Bauer, Phys. Rev. B **37**, 8622 (1988).

[10]T. Kaneko, T. Sasaki, M. Sakuda, R. Yamamoto, T. Nakamura, H. Yamamoto, and S. Tanaka, J. Phys. F **18**, 2053 (1988).

[11]G. Reiss, K. Kapfberger, G. Meier, J. Vancea, and H. Hoffmann, J. Phys. Condens. Matter **1**, 1275 (1989).

[12]C. Dupas, J. P. Renard, J. Seiden, E. Velu, and D. Renard, J. Appl. Phys. **63**, 4300 (1988).

[13]E. Velu, C. Dupas, D. Renard, J. P. Renard, and J. Seiden, Phys. Rev. B **37**, 668 (1988).

[14]M. N. Baibich, J. M. Broto, A. Fert, F. Nguyen Van Dau, F. Petroff, P. Etienne, G. Creuzet, A. Friederich, and J. Chazelas, Phys. Rev. Lett. **61**, 2472 (1988).

[15]G. Binasch, P. Grünberg, F. Saurenbach, and W. Zinn, Phys. Rev. B **39**, 4828 (1989).

[16]F. Saurenbach, J. Barnaś, G. Binasch, M. Vohl, P. Grünberg, and W. Zinn, Thin Solid Films **175**, 317 (1989); the work of J. J. Krebs, P. Lubitz, A. Chaiken, and G. A. Printz [Phys. Rev. Lett. **63**, 1645 (1989)] shows a slightly different thickness range for antiferromagnetic coupling, i.e., 13–25 Å.

[17]M. Kitada and N. Shimizu, Thin Solid Films **158**, 167 (1988).

[18]J. A. J. Lourens, S. Arajs, H. F. Helbig, L. Cheriet, and El-Sayed A. Mehanna, J. Appl. Phys. **63**, 4282 (1988).

[19]E. Dan Dahlberg, K. Riggs, and G. A. Prinz, J. Appl. Phys. **63**, 4270 (1988).

[20]M. Rubinstein, F. J. Rachford, W. W. Fuller, and G. A. Prinz, Phys. Rev. B **37**, 8689 (1988).

[21]P. Grünberg, R. Schreiber, Y. Pang, M. B. Brodsky, and H. Sowers, Phys. Rev. Lett. **57**, 2442 (1986).

[22]F. Saurenbach, U. Walz, L. Hinchey, P. Grünberg, and W. Zinn, J. Appl. Phys. **63**, 3473 (1988).

[23]G. G. Cabrera and L. M. Falicov, Phys. Status Solidi B **61**, 539 (1974); **62**, 217 (1974).

[24]R. E. Camley and J. Barnaś, Phys. Rev. Lett. **63**, 664 (1989).

[25]K. Fuchs, Proc. Cambridge Philos. Soc. **34**, 100 (1938).

[26]H. Sondheimer, Adv. Phys. **1**, 1 (1952).

[27]A. Fert and I. A. Campbell, J. Phys. F **6**, 849 (1976); for a review, see also I. A. Campbell and A. Fert, in *Ferromagnetic Materials*, edited by E. P. Wohlfarth (North-Holland, Amsterdam, 1982) Vol. 3, p. 747.

[28]R. E. Camley and D. R. Tilley, Phys. Rev. B **37**, 3412 (1988).

[29]Z. Tesanovic, M. V. Jaric, and S. Maekawa, Phys. Rev. Lett. **57**, 2760 (1986).

[30]N. Trivedi and N. W. Ashcroft, Phys. Rev. B **38**, 12 298 (1988).